Results in Engineering 27 (2025) 106949

Contents lists available at ScienceDirect

Results in Engineering

journal homepage: www.sciencedirect.com/journal/results-in-engineering

Research paper

# An analytical model for the oscillatory flow in constant cross-section ducts

Hector Sanchez-Izuel, Guillermo Hauke *

*Department of Fluid Mechanics – Instituto de Investigacion en Ingenieria de Aragon (I3A), Escuela de Ingenieria y Arquitectura, Universidad de Zaragoza, 50018 Zaragoza, Spain*

A R T I C L E I N F O

*Keywords:*
Oscillatory flow
Non-circular cross-section ducts
Frequency Reynolds number
Womersly number
Hydraulic diameter
Friction factor
Biological flows
Microfluidics
Hydraulic damper

A B S T R A C T

In this paper, an analytical model for the incompressible laminar mean flow induced by an oscillatory pressure gradient is proposed for *arbitrary* constant cross-section, straight ducts of very large length. With the hydraulic diameter as the characteristic length scale and just one parameter, namely the cross-section loss-coefficient for steady flow, the proposed model provides the modulus and phase of the dimensionless mean flow and volumetric flow rate as a function of the Reynolds frequency number. The model, which is derived from the momentum integral equation using complex algebra, is compared to exact analytical solutions for laminar oscillatory flows. Results for circular, squared, rectangular and triangular cross-sections show that the model accurately reproduces the asymptotic behavior at low and high frequencies, with a reasonable approximation in the intermediate frequency Reynolds number range (1,100), where largest errors occur. The proposed model can be of interest in applied computer programs for engineering, environmental and biological systems that are subject to periodic flows, such as the human circulatory system or the design of hydraulic dampers.

## 1. Introduction

Much attention has been paid to the losses in pipes and the elements of fluid installations under stationary flow [1,2]. However, some systems found in engineering, biology and nature are based on pulsatile and/or oscillatory flows [3].

Note that pulsatile and oscillatory flows are two different types of *periodic flows*, i.e., flows that repeat themselves after a constant period of time, $T$. A *pulsatile* flow can be described as the superimposition of a steady *unidirectional* flow plus a periodically time-varying or *oscillatory* component [4]. The oscillatory component is usually assumed to be *zero mean*, that is, the time-averaged pressure gradient or net flow rate over one period of time, $T$, is zero (see Fig. 1 for an illustration on pulsatile and oscillatory flow). Furthermore, the above flows can be laminar, transitional or turbulent.

This paper focuses on laminar zero-mean oscillatory flows, where an analytical model is proposed for the oscillatory mean flow driven by a sinusoidal pressure gradient. Responses to pulsatile or more complex pressure gradients can be obtained by the sum of the steady and/or oscillatory Fourier modes, which is possible due to the superposition property of the fully developed flow model [4].

Examples of periodic flows can be found in many important applications. This is the case of physiological flows in circulatory systems [5–7], where the study of these types of flows can help understand cardiovascular diseases. In this regard, the study of stenosed channels and arteries has been received much attention in pulsating and oscillating flows (see, for instance, [8–13] and references therein). Oscillatory flows are also present in the design of artificial circulatory systems, like artificial lungs [14], and microfluidic devices, where they can be used to mimic physiological systems to enhance cell cultures, mitigate clog formation, promote mixing and particle separation [15–19]. In engineering applications, this work could have an impact in the design and testing of engine mounts and dampers based on hydraulic circuits to reduce vehicle vibrations [20,21]. In the chemical and bio-industries, cleaning process of fouling deposits and devices may involve pulsed flows [3], as a means to optimize efficiency and avoid chemical additives. In all these areas, the presented model could help derive new models or be embedded in computational models to ease computations, which demonstrates the model relevance across diverse fields.

Note also that, whereas in engineering, environmental and microfluidic applications conduits can be found in any shape including triangular

* Corresponding author.
*E-mail addresses:* hsanchez@unizar.es (H. Sanchez-Izuel), ghauke@unizar.es (G. Hauke).

https://doi.org/10.1016/j.rineng.2025.106949
Received 21 March 2025; Received in revised form 11 August 2025; Accepted 25 August 2025

Available online 3 September 2025

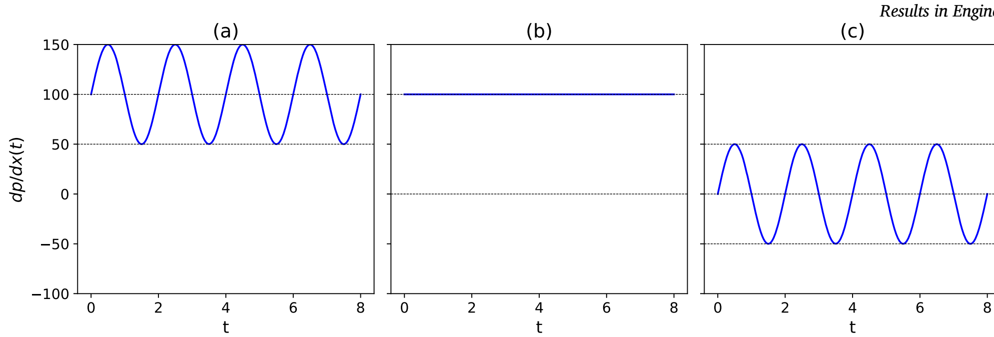


**Fig. 1.** Pulsatile versus oscillatory flow. Example of pressure gradient driving the flow in a duct. (a) Pulsatile flow with nonzero mean. It can be decomposed into (b) Steady flow and (c) Oscillatory flow (with zero-mean).

and rectangular cross-sections, in biology and circulatory systems most conduits typically have approximately circular cross-sections.

Exact analytical solutions of periodic flows in ducts driven by oscillatory pressure gradients have been studied by two techniques: analytical tools and computational or semi analytical methods. Due to the difficulty of finding solutions of the Navier-Stokes equations for general geometries, analytical solutions have been derived for simplified cases, such as conduits of infinite length with unidirectional incompressible velocity distributions, that ignore for instance entrance effects, turbulence and three-dimensionality.

Previous works that deal with analytical solutions for the flow in a circular cylinder and conduits of elliptical cross-sections can be found in [22,4] and references therein. More recent works for rectangular cross-sectional ducts analytical solutions can be found in [23,24] and for triangular cross sections in [25,26]. In particular [25] derives the solution for rectangular isosceles triangular cross-sections based on Fourier series, whereas [26] derives an analytical solution for starting and oscillatory flows in equilateral triangles based on series of eigenfunction solutions. For arbitrary cross-sections, a semi-analytical method is presented in [27]. Computational models and simulations that deal with the transient behavior of ducts can be found for instance in [28,29].

However, present analytical solutions for unidirectional oscillatory flow in straight conduits involve complex and expensive calculations of infinite series, whose solutions may depend on eigenvalue functions [24,26]. In this paper, following the classic assumptions of previous analytical works, an apparently simple model for oscillatory flows is derived, which gives a closed-form expression of the flow rate and mean velocity as a function of the pressure gradient amplitude, that does not require series calculations, and can be of great utility when integrated on models that need inexpensive computations of the flow rate. Another benefit of the present model, which is expressed as a dynamical system of first order, is that it employs the hydraulic diameter as a length scale. This fact could be considered an improvement with respect to the model in [24], where the length scale is the diameter of a circular cylinder having the same steady flow rate as that of the cross-section under study. Furthermore, the present model depends on just one constant parameter, the loss-coefficient of the section in steady flow. Generally, this parameter does not need to be computed, since it is available in the literature for many geometries (see, for instance [2,26,24] and references therein). Finally, this approximate model is valid for any cross-section shape and it is very inexpensive from the computational cost point of view.

Therefore, based on the momentum transport equation, dimensional analysis and the theory of dynamical systems, this paper develops an algebraic model for the oscillatory flow rate of long arbitrary cross-section ducts as a function of frequency. In simulating the transient behavior of the elements of installations, it has been found that the frequency response follows the classic analysis of linear dynamical systems [30]. This behavior can be easily observed in Bode diagrams. Indeed, some exact solutions show that even the series coefficients resemble these functions [26,24].

Bode diagrams represent the frequency response of a system, focusing on the amplitude and the phase of the response in logarithmic scale for the abscissa. One of the advantages of Bode diagrams is that the graphic analysis allows the identification of the nature of the system under study. Thus, it is very useful for the interpretation of empirical results.

The paper is organized as follows. In Section 2, the theory of oscillatory flows for circular cross-section pipes is reviewed. In the third section, dimensional analysis is applied to confirm the relevant dimensionless numbers. Then, the model is developed for the circular geometry to then be extended to non-circular cross-sectional ducts. This section is followed by benchmarking of the model through well-established exact laminar solutions. Finally, the paper ends with the conclusions section.

## 2. Classic analytical solution for circular cross-sectional ducts

For oscillatory laminar incompressible flow inside a circular cross-section rigid long straight pipe driven by a harmonic pressure gradient, [22] presents an analytical solution, which can be used as a benchmark to test models and numerical simulations for the losses in oscillatory flows. This analytical solution assumes unidirectional flow and ignores entrance, turbulence and three-dimensional effects.

Given a pipe of length $L$, radius $R$, in a fluid of density $\rho$, and using complex notation (with $i$ the imaginary unit), the prescribed oscillatory pressure gradient can be written as

$$\frac{\partial p}{\partial x} = -\rho K e^{i\omega t} \tag{1}$$

where $K$ is a constant (equal to $K = \Delta p/(\rho L)$) and $\omega$, the angular velocity (related to the frequency of the motion, $f = 2\pi\omega$). Using the above assumptions, the axial differential momentum equation written in cylindrical coordinates simplifies to

$$\rho \frac{\partial u}{\partial t} = -\frac{\partial p}{\partial x} + \mu \left( \frac{\partial^2 u}{\partial r^2} + \frac{1}{r}\frac{\partial u}{\partial r} \right) \tag{2}$$

where $r$ and $t$ denote respectively the radial and temporal coordinates; $u(r,t)$, the fully developed axial fluid velocity and $\mu$, its fluid dynamic viscosity. After imposing the no-slip boundary condition at the duct wall, $r = R$, and symmetry at $r = 0$, the axial velocity can be written using complex notation and Bessel functions (see [22,4] and references therein)

$$u(r,t) = -i\frac{K}{\omega} e^{i\omega t} \left[ 1 - \frac{J_0(ir\bar{k})}{J_0(iR\bar{k})} \right] \tag{3}$$

where $J_0(z)$ is the zeroth order Bessel function of the first kind and $\bar{k} = \sqrt{i\omega/\nu}$ with $\nu$ the kinematic viscosity. Here, the term $J_0(ir\bar{k})/J_0(iR\bar{k})$ accounts for the variation across the radius. The mean velocity $\bar{u}(t)$, which gives the volumetric flow rate $Q = \bar{u}S$, with $S = \pi R^2$ the cross-sectional area of the duct, can be obtained by integrating $u(r,t)$ across the duct section, yielding

$$\bar{u}(t) = -i\frac{K}{\omega}e^{i\omega t}\left[1 - 2\frac{J_1(iR\bar{k})}{J_0(iR\bar{k})}\right] \tag{4}$$

where $J_1(z)$ is the first order Bessel function of the first kind. In dimensionless form, by reorganizing the constants, the mean velocity (4) can be expressed as

$$\frac{\bar{u}(t)\nu}{KR^2} = -i\frac{1}{\omega R^2/\nu}e^{i\omega t}\left[1 - 2\frac{J_1(\sqrt{-i\omega R^2/\nu})}{J_0(\sqrt{-i\omega R^2/\nu})}\right] \tag{5}$$

For very low and very high frequencies, the asymptotic behavior of the mean velocity is, respectively,

$$\bar{u}(t) = \begin{cases} \frac{KR^2}{8\nu}e^{i\omega t} & \sqrt{\frac{\omega R^2}{2\nu}} << 1 \\ -\frac{iK}{\omega}e^{i\omega t} & \sqrt{\frac{\omega R^2}{2\nu}} >> 1 \end{cases} \tag{6}$$

The oscillating stress at the wall, responsible for the pipe losses, is obtained by differentiating the mean velocity (4) with respect to $r$ at the wall, yielding

$$\tau(t) = \mu\left.\frac{\partial u(r,t)}{\partial r}\right|_{r=R} = -\mu\frac{K\bar{k}}{\omega}e^{i\omega t}\left[\frac{J_1(iR\bar{k})}{J_0(iR\bar{k})}\right] \tag{7}$$

This implies that the stress is slightly phase-delayed with respect to the pressure gradient. Specifically, the complex number involving $\bar{k}$ and the ratio of Bessel functions introduces an imaginary component that shifts the phase of the wall shear stress relative to the real part of the driving pressure gradient.

**Remarks.**

1. As a function of the frequency Reynolds number, $\mathrm{Re}_\omega = \omega R^2/\nu$, the division between low and high frequency corresponds to $\mathrm{Re}_\omega \approx 1$.
2. The square root of the frequency Reynolds number is also called the Womersley number.
3. For low frequencies, $\sqrt{\omega R^2/2\nu} << 1$, the duct behaves as a stationary flow. In this case, the velocity and flow rate respond instantly to the pressure gradient, and are endowed with the same phase, as in Poiseuille flow.
4. For high frequencies, $\sqrt{\omega R^2/2\nu} >> 1$, the volumetric flow rate in the duct tends to zero and to be delayed 90∘ with respect to the pressure gradient.
5. Note that the solution for the mean velocity can be represented as the real part of

$$\bar{u}(t) = \hat{U}e^{i\omega t} \tag{8}$$

with $\hat{U}$ a complex number that depends on $\mathrm{Re}_\omega$.

## 3. Dimensional analysis

Let us apply the dimensional analysis theory [31] to the mean velocity of a pipe in oscillatory flow. Let a pipe of length $L$ and radius $R$, be subject to a periodic pressure difference with amplitude $\Delta p$ and angular velocity $\omega$ in a fluid of density $\rho$ and kinematic viscosity $\nu$. For a given cross-sectional shape, the mean velocity $U$, or $\hat{U}$ in complex notation, produced by the pressure difference is a function of the following variables

$$\hat{U} = f(\Delta p, \omega, R, L, \rho, \nu) \tag{9}$$

According to Buckingham's Pi theorem, adopting $R$, $\rho$ and $\nu$ as fundamental variables yields four dimensionless numbers. Therefore, the above relation $f$ can be expressed as a different dimensionless function $f'$ that depends on

$$\frac{\hat{U}R}{\nu} = f'\left(\frac{L}{R}, \frac{\Delta pR^2}{\rho\nu^2}, \frac{\omega R^2}{\nu}\right) \tag{10}$$

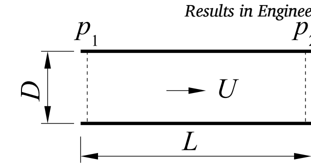


**Fig. 2.** Problem setup.

This new function $f'$ depends only on three variables instead of five. The third number is the Reynolds number based on angular velocity,

$$\mathrm{Re}_\omega = \frac{\omega R^2}{\nu} \tag{11}$$

which will be termed the frequency Reynolds number.

From the analytical solution of Section 2, for a duct of cross-sectional area $S$, it can be concluded that the volumetric flow rate $Q = US$ depends linearly with respect to the pressure gradient and it is inversely proportional to the pipe length $L$. Therefore, in Eq. (10) the dependency of $Q$ or $U$ can be linearized with respect to the pressure difference $\Delta p$ and $R/L$, resulting in

$$\frac{\hat{U}R}{\nu} = \frac{R}{L}\,\frac{\Delta pR^2}{\rho\nu^2}\,\mathrm{C_q}(\frac{\omega R^2}{\nu}) \tag{12}$$

Finally, this implies that the dimensionless flow rate in a duct can be expressed as a function of just one dimensionless number, namely, the frequency Reynolds number,

$$\boxed{\frac{\hat{U}\ \mu\mathrm{L}}{\Delta pR^2} = \mathrm{C_q}(\mathrm{Re}_\omega)} \tag{13}$$

As a consequence, the dimensionless complex mean velocity (or volumetric flow rate) depends only on the shape of the cross-section and $\mathrm{Re}_\omega$, i.e., the dimensionless frequency. This result is in agreement with the analytical solution (5).

## 4. A model of oscillatory flow for circular cross-sections

The transient integral momentum equation that governs the fully-developed mean velocity $U(t)$ in a straight pipe of length $L$ and circular constant cross-section $S$ under a pressure difference $p_2 - p_1$ (see Fig. 2) can be written in the axial direction for laminar flow as [31],

$$\rho\frac{\mathrm{d}U}{\mathrm{d}t}LS = (p_1 - p_2)S - 32\frac{\mu\mathrm{L}}{D^2}US \tag{14}$$

For oscillatory flow, using complex variable, let

$$p_1(t) - p_2(t) = (\hat{p}_1 - \hat{p}_2)\,e^{i\omega t} = \Delta p\,e^{i\omega t} \tag{15}$$

$$U(t) = \hat{U}\,e^{i\omega t} \tag{16}$$

Note that $\hat{U}$ is a complex variable that has information about the modulus of the mean velocity and its phase with respect to the pressure gradient. Substituting into Eq. (14) yields,

$$i\omega\rho L\hat{U} = (\hat{p}_1 - \hat{p}_2) - 32\frac{\mu\mathrm{L}}{D^2}\hat{U} \tag{17}$$

The pressure gradient and the previously defined constant $K$ can be identified as

$$K = -\frac{1}{\rho}\frac{\mathrm{d}\hat{p}}{\mathrm{d}x} = \frac{\hat{p}_1 - \hat{p}_2}{\rho L} = \frac{\Delta p}{\rho L} \tag{18}$$

Operating, the mean velocity in the pipe can be expressed as

$$\hat{U} = \frac{K}{i\omega + \frac{8\nu}{R^2}} \tag{19}$$

which, in dimensionless form, becomes

$$\frac{\hat{U}\nu}{KR^2} = \frac{1}{i\frac{\omega R^2}{\nu} + 8} \tag{20}$$

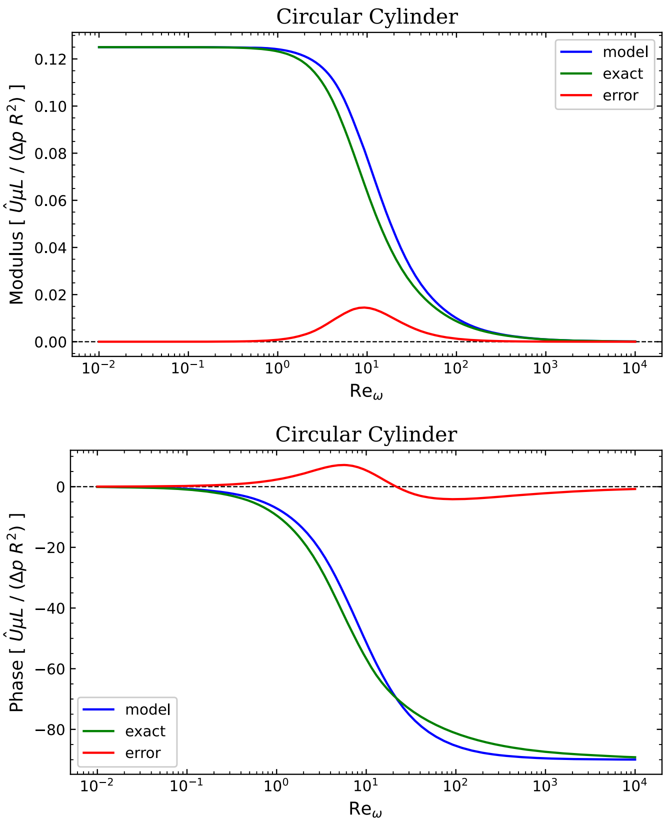


**Fig. 3.** Bode diagram showing the dimensionless mean velocity behavior (modulus and phase) as a function of frequency Reynolds number, $\mathrm{Re}_\omega$, in a circular duct. Analytical solution of Womersley [22] and present model (21).

As a function of the frequency Reynolds number $\mathrm{Re}_\omega = \omega R^2/\nu$ and the pressure gradient $\Delta p/L$, the above expression can be written as

$$\frac{\hat{U}\ \mu\mathrm{L}}{\Delta p R^2} = \frac{1}{i\ \mathrm{Re}_\omega + 8} \tag{21}$$

Fig. 3 (obtained with Python [32]) depicts the dimensionless mean flow response of the exact solution and the present model as a function of dimensionless frequency in a Bode diagram, showing a very similar response. Indeed, in control theory this response corresponds to a linear system of first order [24]. In particular, the top plot analyzes the dimensionless mean velocity modulus as a function of frequency whereas the bottom plot shows the phase of the mean velocity. The red line depicts the error of the present model with respect to the exact analytical solution.

**Remarks.**

1. The asymptotic behavior of the model coincides with that of the analytical solution, namely:

$$\lim_{\omega\to 0} \hat{U} = \frac{K R^2}{8\nu} \tag{22}$$

$$\lim_{\omega\to \infty} \hat{U} = -\frac{iK}{\omega} \tag{23}$$

In dimensionless form,

$$\lim_{\omega\to 0} \frac{\hat{U}\ \mu\mathrm{L}}{\Delta p R^2} = \frac{1}{8} \tag{24}$$

$$\lim_{\omega\to \infty} \frac{\hat{U}\ \mu\mathrm{L}}{\Delta p R^2} = -\frac{i}{\mathrm{Re}_\omega} \tag{25}$$

2. The model's mean velocity modulus and phase are practically identical as the exact velocity modulus for the whole range of frequencies.
3. For low frequencies, the modulus of the mean fluid velocity is in phase with the pressure gradient, and the flow behaves as a steady flow.
4. For high frequencies, the modulus of the mean fluid velocity tends to zero, while its phase tends to a delay of 90°.
5. Therefore, Fig. 3 shows that the proposed model matches the exact solution for the limiting cases of zero and infinite frequency. The zero frequency case corresponds to a very slowly changing flow, where the steady friction factor employed in the present model exactly represents the flow solution. In the high-frequency regime, the velocity and flow rate tend to zero, so the friction factor data has little impact on the fluid flow. The error between the model and the exact solution is highest in the medium regime of Reynolds numbers (1, 100), where the unsteadiness and inertia of the flow are significant. In this range, the steady friction factor departs from the exact unsteady one.

## 5. Extension of the model to non-circular cross-sections

Equation (14) can be extended to non-circular cross-sections introducing the hydraulic diameter of the pipe [2],

$$D_h = \frac{4S}{\mathbb{P}} \tag{26}$$

where $S$ is the cross-sectional area and $\mathbb{P}$ is the wetted perimeter, that is, the length of the perimeter of the cross-section that is in contact with the fluid and, therefore, subject to friction. For laminar flow, the steady friction factor based on the hydraulic diameter can be written as

$$\lambda = \frac{(f\,Re)}{Re_{D_h}} \tag{27}$$

where $(f\,Re)$ is a constant dependent on the cross-sectional shape [2].

In this case, the momentum equation in the axial direction, Eq. (14), becomes

$$\rho \frac{\mathrm{d}U}{\mathrm{d}t} L S = (p_1 - p_2) S - \frac{(f\,Re)}{2} \frac{\mu\mathrm{L}}{D_h^2} U S \tag{28}$$

After some algebra and defining the radius as half the hydraulic diameter, $R = D_h/2$, one obtains

$$\boxed{\frac{\hat{U}\ \mu\mathrm{L}}{\Delta p R^2} = \frac{1}{i\ \mathrm{Re}_\omega + \frac{(f\,Re)}{8}}} \tag{29}$$

**Remarks.**

1. Equation (29) can be used for any cross-sectional shape, as it depends on its $(f\,Re)$ value, the steady loss coefficient. The asymptotics for small and large frequencies are:

$$\lim_{\omega\to 0} \frac{\hat{U}\ \mu\mathrm{L}}{\Delta p R^2} = \frac{8}{(f\,Re)} \tag{30}$$

$$\lim_{\omega\to \infty} \frac{\hat{U}\ \mu\mathrm{L}}{\Delta p R^2} = -\frac{i}{\mathrm{Re}_\omega} \tag{31}$$

2. Note that for the circular cylinder, $(f\,Re) = 64$ and Eq. (21) is recovered.
3. Observe also that the dimensionless mean flow depends solely on *one variable* –the dimensionless frequency number, $\mathrm{Re}_\omega$– and *one parameter:* the steady friction factor of the cross-section, $(f\,Re)$. Also, the higher the friction factor of the cross-section, the smaller the mean flow modulus.

**Table 1**
Steady friction factors in straight ducts for several cross-sections [2].

| Cross-section | $(f\,Re)$ |
|---|---|
| Circular | 64.00 |
| Concentric cylinders with aspect ratio 0.6 | 95.59 |
| Concentric cylinders with aspect ratio 0.4 | 94.71 |
| Squared | 56.91 |
| Rectangular with aspect ratio 0.5 | 62.19 |
| Rectangular with aspect ratio 0.25 | 72.93 |
| Equilateral triangular | 51.10 |
| Isosceles triangular, $\alpha = 30°$ | 53.30 |

4. Although the model appears simple compared to other exact analytical solutions and uses the steady loss coefficient of the cross-section, it gives quite remarkable results as will be shown next.
5. This model can be very useful when integrated in more complex models that need an inexpensive expression of the flow rate or the mean velocity as a function of time [20,33,34].
6. Table 1 shows $(f\,Re)$ for typical cross-sections.

## 6. Application examples of the model to non-circular cross-sections

In this section, the behavior of the present model, given by (29), is compared to well-established analytical solutions in the laminar regime for ducts with squared, rectangular and equilateral triangular cross-sections.

The results are presented in dimensionless form as Bode diagrams, which display the magnitude and phase of the sinusoidal mean flow induced by the prescribed pressure gradient frequency (or angular velocity $\omega$). The dimensionless frequency is represented by the frequency Reynolds number. Thus, as the horizontal axis spans from zero to large values of the frequency Reynolds number, the corresponding frequency is also scanned from zero to large values. For the same reason, dimensional analysis dictates that the results are valid for any duct size, as they depend solely on the cross-sectional shape. All plots in this section were generated using Python [32].

### 6.1. Squared cross-section

It is instructive to compare the proposed model with the solution of Urata [24] for arbitrary rectangular aspect ratios, whose length scale is based on the diameter of a circular pipe with equivalent volumetric flow rate. While accurate, this method can be cumbersome in practical applications. In contrast, the present model uses the hydraulic diameter as length scale, a readily available geometric property with a direct physical interpretation.

As an example, Fig. 4 shows the Bode diagram for the present model applied to a *squared cross-section* duct, compared to Urata's analytical solution. In this geometry, $(f\,Re) = 56.91$, $\mathbb{P} = 4a$, $S = a^2$ and $D_h = a = 2R$, with $a$ the side of the section [2]. Thus, the model simplifies to:

$$\frac{\hat{U}\ \mu L}{\Delta p R^2} = \frac{1}{i\ \mathrm{Re}_\omega + 7.114} \tag{32}$$

In particular, Fig. 4 compares the exact and modeled mean flow solutions for square cross-section ducts as functions of dimensionless frequency. The top plot shows the dimensionless velocity modulus, while the bottom plot presents its phase relative to the pressure gradient. The red line depicts the error of the present model and the exact analytical solution. Once again, we observe that the oscillatory flow behaves like a first-order dynamical system, and the model matches the exact solution at both very low and high frequencies. The largest discrepancy between the model and the analytical solution occurs in the intermediate range, specifically for frequency Reynolds numbers between 1 and 100, where

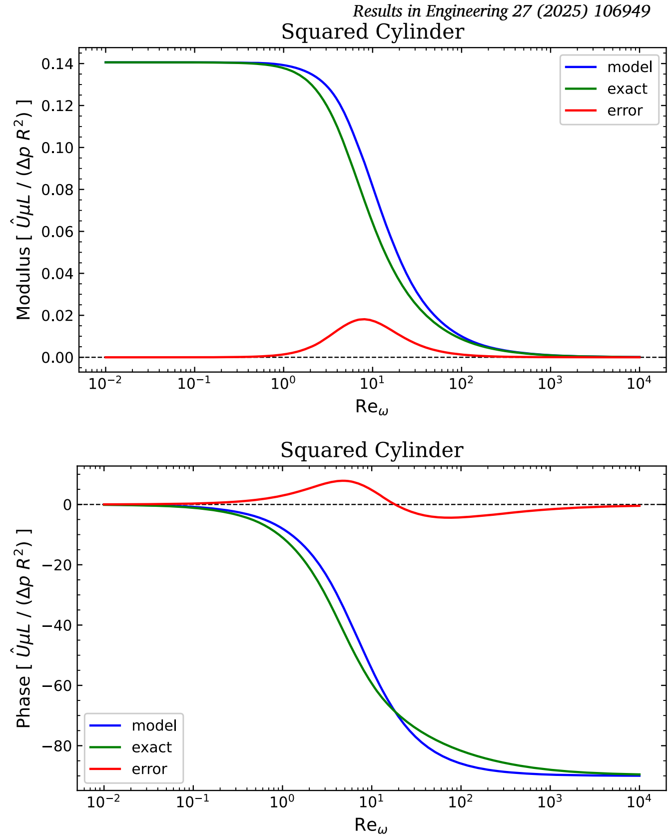


**Fig. 4.** Bode diagram showing the modulus and phase of the dimensionless mean flow in a squared cross-section duct as a function of the frequency Reynolds number $\mathrm{Re}_\omega$. The present model (32) is compared to Urata's analytical solution [24].

the assumptions underlying the model begin to diverge from the exact dynamics.

### 6.2. Rectangular cross-section

For the case of a rectangular cross-section with an aspect ratio 0.5, $(f\,Re) = 62.19$, $\mathbb{P} = 3a$, $S = a^2/2$, and $D_h = 2a/3 = 2R$, with $a$ the longest side of the section [2]. Fig. 5 shows the Bode diagram response of the proposed model compared with the analytical solution of Urata [24]. Thus, in this case:

$$\frac{\hat{U}\ \mu L}{\Delta p R^2} = \frac{1}{i\ \mathrm{Re}_\omega + 7.774} \tag{33}$$

Again, Fig. 5 compares the exact and modeled mean flow solutions for a rectangular cross-section duct as functions of dimensionless frequency. The same comments made for the square cross-section apply here.

### 6.3. Equilateral triangular cross-section

For the case of an equilateral triangular cross-section, $(f\,Re) = 51.10$, $\mathbb{P} = 3a$, $S = 0.4330\,a^2$ and $D_h = 0.5774\,a$, with $a$ the side of the triangle [2]. Accordingly, the present model yields:

$$\frac{\hat{U}\ \mu L}{\Delta p R^2} = \frac{1}{i\ \mathrm{Re}_\omega + 6.388} \tag{34}$$

In this case, Fig. 6 compares the present model with the exact solution presented in [26], which is obtained using a series expansion in terms of eigenvalues and eigenvectors.

Fig. 6 compares the exact and modeled mean flow solutions for the equilateral triangular cross-section duct as functions of dimensionless

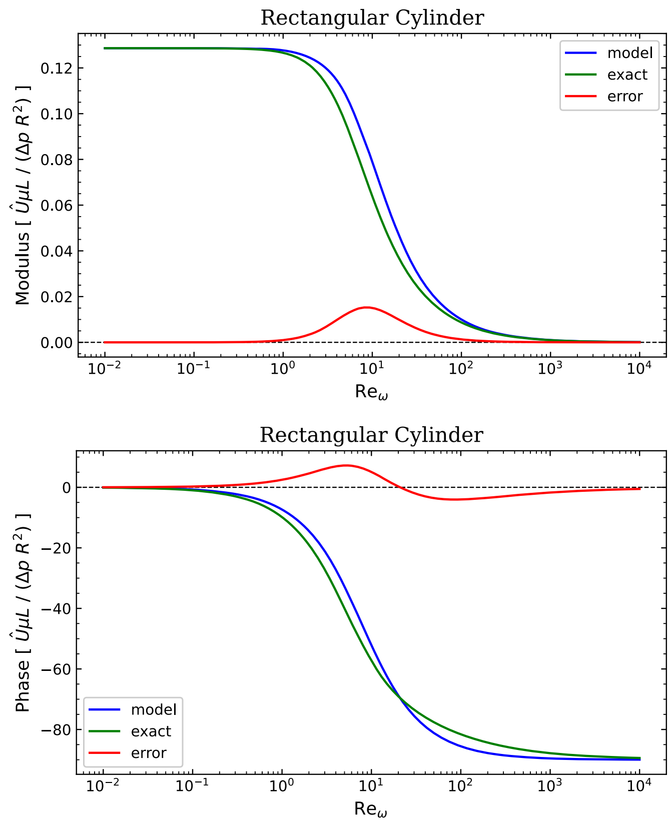


**Fig. 5.** Bode diagram showing the modulus and phase of the dimensionless mean flow in a rectangular cross-section cylinder with aspect ratio 0.5 as a function of the frequency Reynolds number, $\mathrm{Re}_\omega$. The present model (33) is compared to Urata's analytical solution [24].

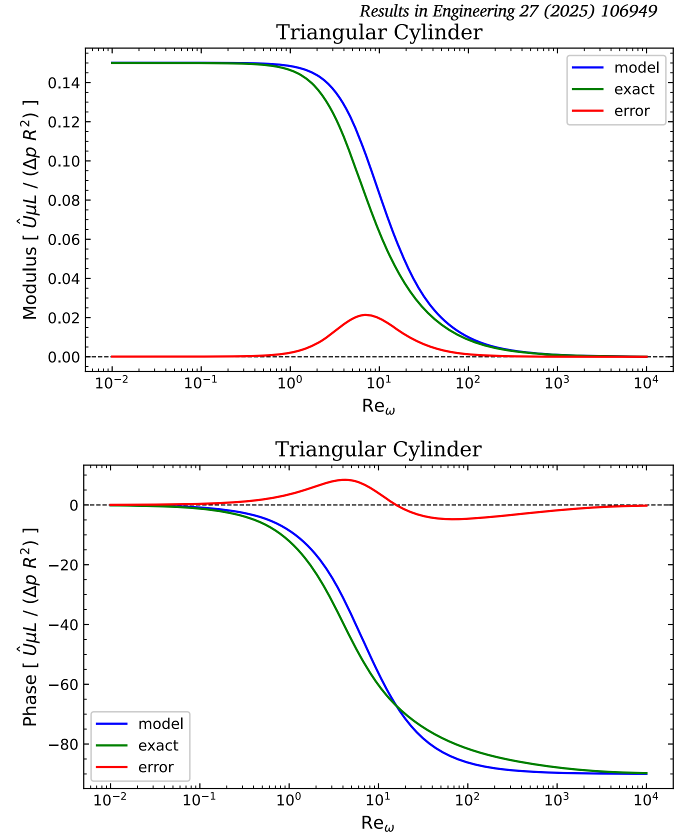


**Fig. 6.** Bode diagram showing the modulus and phase of the dimensionless mean flow in an equilateral triangular cross-section cylinder as a function of frequency Reynolds number, $\mathrm{Re}_\omega$. The present model (34) is compared to Wang's analytical solution [26].

frequency. The top plot presents the dimensionless velocity modulus, while the bottom plot shows the corresponding phase relative to the pressure gradient. The red line indicates the error of the present model relative to the exact analytical solution. As noted earlier, the oscillatory flow behaves like a first-order dynamical system. The model is accurate for very low and very high frequencies, with the largest error occurring in the intermediate frequency Reynolds number range $(1, 100)$.

## Conclusions

A model for flow in long ducts of arbitrary constant cross-section under an oscillatory pressure gradient has been developed using the integral momentum equation, dimensional analysis and the theory of linear dynamical systems. The model, based on complex variable theory, expresses the dimensionless mean flow (or volumetric flow rate) as a function of the dimensionless frequency and a single parameter, namely $(f\,Re)$, the steady-state friction factor for laminar flow. The characteristic length scale used is the hydraulic diameter, which naturally leads to the definition of a frequency Reynolds number.

It has been shown that the oscillatory flow rate and mean velocity behave as a first-order linear dynamical system. For low frequencies, the mean velocity reaches its maximum and is in phase with the applied pressure gradient, behaving as a quasi-steady flow. This explains why using the steady friction factor in the model yields good agreement with the analytical solution. At high frequencies, the flow rate tends toward zero and lags the pressure gradient by 90°, which accounts for the model's accuracy in that regime as well. Consequently, the greatest error occurs in the intermediate-frequency regime, for Reynolds frequency numbers in the interval $(1, 100)$.

In dimensionless form, the modeled mean flow depends solely on the dimensionless frequency of the driving pressure gradient and the steady friction factor of the cross-section. It has been shown that a larger friction factor corresponds to a smaller flow rate.

The model has been compared to well-established analytical solutions, demonstrating reasonable accuracy. It is therefore potentially useful in applied models and computational tools for engineering and biological systems that are subject to periodic flows.

This model has practical applications in both engineering and biological contexts. In engineering, it can be integrated into the design of hydraulic shock absorbers for automotive engine mounts and suspension systems, where oscillatory flows are induced by periodic vibrations [20,21]. It is also applicable to microfluidic devices, where precise control of oscillatory flow in non-circular channels enhances mixing and pumping efficiency. In biomedical applications, the model can support simulations of blood flow in small vessels, stenosed arteries or artificial circulatory devices–such as total artificial lungs–where oscillatory components influence gas exchange [14]. By providing a computational inexpensive yet accurate tool, the model enables real-time analysis for such applications.

## CRediT authorship contribution statement

**Hector Sanchez-Izuel:** Writing – original draft, Visualization, Investigation. **Guillermo Hauke:** Writing – review & editing, Writing – original draft, Investigation, Funding acquisition, Conceptualization.

## Funding

The authors gratefully acknowledge the financial support through the project PID2022-138572OB-C44, funded by MCIN/AEI/10.13039/501100011033/FEDER, UE and Gobierno de Aragón/FEDER-UE (Grupo de Referencia de Tecnologias Fluidodinamicas DGA-T32_23R).

## Declaration of competing interest

The authors declare the following financial interests/personal relationships which may be considered as potential competing interests: Guillermo Hauke reports financial support was provided by Ministry of Science Technology and Innovations, grant number PID2022-138572OB-C44. Guillermo Hauke reports financial support was provided by Government of Aragon, Grupo de Referencia de Tecnologias Fluidodinamicas DGA-T32_23R. If there are other authors, they declare that they have no known competing financial interests or personal relationships that could have appeared to influence the work reported in this paper.

## Acknowledgements

The authors are grateful to F. Alcrudo and M.H. Doweidar for their valuable discussions and insights.

## Data availability

No data was used for the research described in the article.

## References

[1] I. Idel'chik, Handbook of Hydraulic Resistance, 1966.
[2] F. White, Fluid Mechanics, 7th edition, Mc Graw Hill, 2011.
[3] R. Absi, Oscillatory and pulsatile flows in environmental, biological and industrial applications, in: 8th International Conference on Fluid Mechanics (ICFM8), 2018, pp. 1–9.
[4] M. Zamir, The Physics of Pulsatile Flow, Biomedical, Springer, 2000.
[5] T.J.R. Hughes, J. Lubliner, On the one-dimensional theory of blood flow in the larger vessels, Math. Biosci. 18 (1973) 161–170.
[6] J. Wan, B. Steele, S.A. Spicer, S. Strohband, G.R. Feijóo, T.J. Hughes, C.A. Taylor, A one-dimensional finite element method for simulation-based medical planning for cardiovascular disease, Comput. Methods Biomech. Biomed. Eng. 5 (3) (2002) 195–206.
[7] B. Soni, A. Suri, A. Nayak, A. Miguel, Simplified lumped parameter model for oscillatory flow in an elastic tube: a hierarchical approach, J. Fluids Eng. (2022).
[8] R. Mittal, S.P. Simmons, F. Najjar, Numerical study of pulsatile flow in a constricted channel, J. Fluid Mech. 485 (2003) 337–378, https://doi.org/10.1017/S002211200300449X.
[9] S.S. Varghese, S.H. Frankel, P.F. Fischer R, Direct numerical simulation of stenotic flows. Part 2. Pulsatile flow, J. Fluid Mech. 582 (2007) 281–318, https://doi.org/10.1017/S0022112007005836.
[10] M. Paul, M. Molla, Investigation of physiological pulsatile flow in a model arterial stenosis using large-eddy and direct numerical simulations, Appl. Math. Model. 36 (9) (2012) 4393–4413, https://doi.org/10.1016/j.apm.2011.11.065.
[11] M.M. Molla, B.-C. Wang, D.C.S. Kuhn, Numerical study of pulsatile channel flows undergoing transition triggered by a modelled stenosis, Phys. Fluids 24 (12) (2012) 121901, https://doi.org/10.1063/1.4771604.
[12] K. Jain, Transition to turbulence in an oscillatory flow through stenosis, Biomech. Model. Mechanobiol. 19 (9) (2020) 113–131.
[13] S. Mirfendereski, J.S. Park, Direct numerical simulation of a pulsatile flow in a stenotic channel using immersed boundary method, Eng. Rep. 4 (1) (2022) e12444, https://doi.org/10.1002/eng2.12444.
[14] A. Qamar, R. Seda, J. Bull, Pulsatile flow past an oscillating cylinder, Phys. Fluids 23 (4) (2011) 041903.
[15] B. Dincau, E. Dressaire, A. Sauret, Pulsatile flow in microfluidic systems, Small 16 (9) (2020) 1904032–18.
[16] L. Ding, Shear dispersion of multispecies electrolyte solutions in the channel domain, J. Fluid Mech. 970 (2023) A27, https://doi.org/10.1017/jfm.2023.626.
[17] T. Karmakar, S. Barik, G.P. Raja Sekhar, Multi-scale analysis of concentration distribution in unsteady Couette-Poiseuille flows through a porous channel, Proc. R. Soc. A 479 (2023) 20220494, https://doi.org/10.1098/rspa.2022.0494.
[18] N. Poddar, G. Saha, K.K. Mondal, S. Dhar, B.S. Mazumder, Effect of phase exchange kinetics on Taylor dispersion of chemically reactive solutes in an oscillatory magnetohydrodynamics flow between two parallel plates, Phys. Fluids 36 (5) (2024) 053601, https://doi.org/10.1063/5.0203246.
[19] W. Jiang, G. Chen, Transient dispersion in oscillatory flows: auxiliary-time extension method for concentration moments, arXiv:2507.01870, https://arxiv.org/abs/2507.01870, 2025.
[20] G. Kim, R. Singh, A study of passive and adaptive hydraulic engine mount systems with emphasis on non-linear characteristics, J. Sound Vib. 179 (3) (1995) 427–453.
[21] L. Fredette, S. Rath, R. Singh, Nonlinear fluid damping models for hydraulic bushing under sinusoidal or transient excitation, Proc. Inst. Mech. Eng. Part D, J. Automob. Eng. 233 (3) (2019) 595–604.
[22] J.R. Womersley, Method for the calculation of velocity, rate of flow and viscous drag in arteries when the pressure gradient is known, J. Physiol. 127 (3) (1955) 553–563.
[23] A. Tsimpoukis, D. Valougeorgisa, Pulsatile pressure driven rarefied gas flow in long rectangular ducts, Phys. Fluids 30 (2018) 047104.
[24] E. Urata, The frequency response of rectangular ducts, J. Mech. Eng. Sci. 229 (6) (2015) 1103–1111.
[25] S. Tsangaris, N.W. Vlachakis, Exact solution of the Navier-Stokes equations for the oscillating flow in a duct of a cross-section of right-angled isosceles triangle, Z. Angew. Math. Phys. 54 (6) (2003) 1094–1100.
[26] C.Y. Wang, Exact solutions for starting and oscillatory flows in an equilateral triangular duct, J. Fluids Eng. 138 (8) (2016).
[27] S. Ray, F. Durst, Semianalytical solutions of laminar fully developed pulsating flows through ducts of arbitrary cross sections, Phys. Fluids 16 (12) (2004) 4371–4385.
[28] A. Yakhot, M. Arad, G. Ben-Dor, Pulsatile flow in a rectangular duct, Int. J. Numer. Methods Fluids 29 (1999) 935–950.
[29] A. Adamkowski, Analysis of transient flow in pipes with expanding or contracting sections, J. Fluids Eng. 125 (2003) 716–722.
[30] K. Ogata, Modern Control Engineering, Pearson, 2009.
[31] G. Hauke, An Introduction to Fluid Mechanics and Transport Phenomena, Springer, 2008.
[32] Python Software Foundation. [link], https://www.python.org/.
[33] A. Geisberger, A. Khajepour, M. Golnaraghi, Non-linear modelling of hydraulic mounts: theory and experiment, J. Sound Vib. 249 (2002) 371–397, https://doi.org/10.1006/jsvi.2001.3860.
[34] S. He, R. Singh, Approximate step response of a nonlinear hydraulic mount using a simplified linear model, J. Sound Vib. 299 (2007) 656–663.